Fabrication of electron beam deposited tip for atomic-scale atomic force microscopy in liquid

Significant improvements in stability and reproducibility of atomic-scale atomic force microscopy in liquid

S M R Akrami[1], H Nakayachi[1], T Watanabe-Nakayama[2], H Asakawa[2] and T Fukuma[1,2,3]

[1] Division of Electrical Engineering and Computer Science, Kanazawa University, Kakuma-machi, Kanazawa 920-1192, Japan

[2] Bio-AFM Frontier Research Center, Kanazawa University, Kakuma-machi, Kanazawa 920-1192, Japan

[3] ACT-C, Japan Science and Technology Agency, Honcho 4-1-9, Kawaguchi 332-0012, Japan

E-mail: fukuma@staff.kanazawa-u.ac.jp

Abstract. Recent advancement of dynamic-mode atomic force microscopy (AFM) for liquid-environment applications enabled atomic-scale studies on various interfacial phenomena. However, instabilities and poor reproducibility of the measurements often prevent systematic studies. To solve this problem, we have investigated the effect of various tip treatment methods for atomic-scale imaging and force measurements in liquid. The tested methods include Si coating, Ar plasma, Ar sputtering and UV/O_3 cleaning. We found that all the methods provide significant improvements in both the imaging and force measurements in spite of the tip transfer through the air. Among the methods, we found that the Si coating provides the best stability and reproducibility in the measurements. To understand the origin of the fouling resistance of the cleaned tip surface and the difference between the cleaning methods, we have investigated the tip surface properties by x-ray photoelectron spectroscopy and contact angle measurements. The results show that the contaminations adsorbed on the tip during the tip transfer through the air should desorb from the surface when it is immersed in aqueous solution due to the enhanced hydrophilicity by the tip treatments. The tip surface prepared by the Si coating is oxidized when it is immersed in aqueous solution. This creates local spots where stable hydration structures are formed. For the other methods, there is no active mechanism to create such local hydration sites. Thus, the hydration structure formed under the tip apex is not necessarily stable. These results reveal the desirable tip properties for atomic-scale AFM measurements in liquid, which should serve as a guideline for further improvements of the tip treatment methods.

PACS numbers: 07.79.Lh, 68.37.Ps

1. Introduction

Atomic force microscopy (AFM)[1] has a unique capability of imaging atomic-scale structures of insulating materials as well as conductive ones in liquid. Owing to this capability, the method has been used for subnanometer-scale studies on various materials including minerals[2, 3, 4, 5], biological systems[6, 7, 8, 9, 10, 11, 12] and metal surfaces[13]. For such subnanometer-scale applications in liquid, contact-mode AFM has traditionally been used[2, 6]. However, the method has limitations in its application range. It is often difficult to image isolated molecules weakly bound to a substrate due to a friction force caused by a tip scan. In addition, operating conditions that allow true atomic-resolution imaging is limited. Thus, non-periodic atomic-scale surface features are often averaged out in an obtained image.

Recently, there has been significant advancement in liquid-environment dynamic-mode AFM. Atomic-scale measurements by dynamic-mode AFM have traditionally been performed only in vacuum using frequency modulation AFM (FM-AFM)[14, 15, 16]. In 2005, Fukuma *et al.* enabled operation of FM-AFM in liquid with true atomic resolution[3]. One of the major improvements that brought this breakthrough was reduction of cantilever oscillation amplitude (A: peak-to-zero value) to less than 0.5 nm. Such small amplitude operation enhances sensitivity to a short-range interaction force that is responsible for the formation of atomic-scale image contrasts[17, 18]. Subsequently, the effectiveness of the small amplitude operation was also demonstrated in phase modulation and amplitude modulation AFM[19, 20]. Another technique proposed for high-resolution imaging is bimodal AFM[21]. In the method, a cantilever is oscillated at two different frequencies corresponding to the first and second vibration modes. The oscillation amplitude of the second mode is typically set at a small value. Thus, amplitude and phase images of the second vibration mode often show atomic-scale contrasts[10].

These developments of the operation techniques have significantly improved spatial resolution of dynamic-mode AFM. In addition, recent development of ultra-small cantilevers has remarkably improved force sensitivity of dynamic-mode AFM[22, 9]. Thus, force sensitivity and spatial resolution of the present dynamic-mode AFM are sufficient for most of the atomic-scale applications. In contrast, stability and reproducibility of these techniques are often insufficient for practical applications. Even for an imaging of a standard sample such as a cleaved mica surface, we often observe contrast changes during one frame scan. Furthermore, atomic-scale contrasts observed in one image is not necessarily reproduced in another image. Such instabilities and poor reproducibility have hindered systematic studies on various interfacial phenomena.

These problems originate from instabilities and poor reproducibility of the tip apex conditions. For FM-AFM experiments in vacuum, it has been common to clean the tip apex by ion beam sputtering. However, for liquid-environment applications, we should transfer the cleaned tip to a liquid environment through the air. Thus, it should be difficult to keep the tip apex atomically clean throughout the transfer process. In

the meanwhile, previous studies suggested that even simple surface treatment methods using plasma, UV/O_3 or piranha solution are effective at least for nanoscale AFM measurements[23, 24, 25]. In these studies, the authors suggested the importance of the improved tip cleanliness and hydrophilicity for their AFM measurements. However, these results do not necessarily ensure that the methods are also effective for atomic-scale AFM measurements, where atom-to-atom interactions predominantly contribute to the formation of image contrasts.

In this study, we have investigated the effect of various tip treatment methods for atomic-scale imaging and force measurements in liquid. The methods that we tested include Si coating, Ar plasma, Ar sputtering and UV/O_3 cleaning. Based on the results, we clarify which method gives the best performance in atomic-scale AFM measurements. In addition, we investigate the surface properties of the tip before and after the treatments by X-ray photoelectron spectroscopy (XPS) and contact angle (CA) measurements. From the results, we discuss origins for the different performance obtained by the different methods and clarify the cleaning mechanism.

2. Experimental details

2.1. Tip treatment methods

In this study, we used Si cantilever with backside Au coating (PPP-NCHAuD, Nanoworld). The nominal spring constant (k) of the cantilever is 42 N/m while typical resonance frequency (f_0) and Q factor in liquid are 140 kHz and 8, respectively. The nominal tip radius (R_t) is less than 8 nm.

In the Si coating method, we coated the tip with Si by dc sputter coater (K575XD, Emitech). The thickness of the Si coat was set at 30 nm. We used this thickness to ensure that the tip apex is completely covered with the deposited Si film.

For the Ar plasma cleaning, we used a plasma cleaner from Sanyu Electronics (SC-701). We found that the Ar plasma cleaning with a typical operating condition can severely damage a cantilever. By imaging the cleaned cantilever with an optical microscope, we found that the edges of its fixed end are etched by the plasma. Thus, we adjusted the bias voltage and the inlet gas pressure just as high as required for maintaining the plasma. In addition, we covered the cantilever with Ta plate to suppress the electric field applied to the cantilever surface. Under this condition, surface damage caused by the cleaning is negligible.

In the Ar sputtering method, we used an ion source from SPECS (IQE 11/35) installed in a custom-made vacuum chamber. The cantilever was placed 5 cm away from the ion source. The base pressure before the sputtering was 5×10^{-6} Pa. We introduced Ar gas into the chamber such that the pressure reaches 1.3×10^{-4} Pa. The sputtering was performed for 5 min with an acceleration voltage of 0.6 kV.

For the UV/O_3 cleaning, we used a UV/O_3 cleaner from BioForce Nanoscience (ProCleaner Plus). The cantilever was placed on a large quartz crystal and processed

for 5 min. We found that further processing results in a significant increase of the tip radius (R_t) as discussed in the following section. Immediately after the processing, we immersed the cantilever into water for a few seconds to discharge the surface. Without this process, the surface is soon contaminated during the transfer through the air.

In the previous studies[23, 25, 26, 27], tip treatment methods using acidic solution (i.e. piranha solution) were successfully used. However, in our preliminary experiments, we found that acidic solution can damage the Au backside coating of a cantilever. Although there may be a moderate condition that can only eliminate surface contaminations, we were not able to find it in the preliminary experiments. Thus, here we compare the major dry processes that have been used for the tip treatments.

2.2. AFM measurements

AFM Measurements were performed by custom-built FM-AFM with an ultra-low noise cantilever deflection sensor[28, 29, 30]. A commercially available AFM controller (ARC2, Asylum Research) was used for controlling the AFM and recording data. A cantilever was oscillated at its resonance frequency using a phase-locked loop (PLL) circuit (OC4, SPECS). The PLL circuit was also used for detecting frequency shift (Δf) of the cantilever resonance. The FM-AFM imaging was performed with a constant Δf mode.

To evaluate the effect of the tip treatments, we performed atomic-scale imaging and force measurements on a cleaved mica surface in phosphate buffered saline (PBS) solution. This model system has widely been used for demonstrating atomic-resolution imaging capability of various dynamic-mode AFM techniques[3, 19, 20]. To evaluate the reproducibility of the results, we performed three experiments for each treatment method. For every experiment, we used a new cantilever.

The experimental procedure for one experiment is as follows. Immediately after a tip treatment, we transferred the cleaned tip to an imaging solution. After we made a tip approach to a cleaved mica surface, we performed 10 frame imaging with typical conditions for atomic-resolution FM-AFM imaging in liquid (scan size: 8×8 nm^2, tip velocity: 223 nm/s, cantilever oscillation amplitude (A): 0.25 nm, frequency shift (Δf): 800 Hz). After the imaging, we measured 10 Δf curves with typical conditions for hydration force measurements by FM-AFM (tip velocity: 1 nm/s, sample rate: 1 kHz, measurement bandwidth (B): 10 Hz, A: 0.1 nm). After collecting the 10 Δf curves, we changed A from 0.1 to 0.25 nm and collected another 10 curves. This amplitude value is the same as used for the imaging. Thus, the measured Δf curves allow us to estimate the Δf slope, on which we made a tip-sample distance regulation during the imaging. Note that we did not change any parameters during the imaging and force measurements. Therefore, the obtained data may not be obtained with the optimal conditions. However, this ensures that the data is free from the influence of the operator's experimental skill.

2.3. Other evaluation methods

Scanning electron microscopy (SEM) imaging was performed with field emission SEM from Elionix (ERA-8000FE). An acceleration voltage and a working distance were set at 15 kV and 11 mm. Note that the cantilevers imaged by SEM were not used for the AFM measurements. Namely, all the AFM experiments were performed just after the tip treatment without SEM imaging.

XPS measurements were performed by Sigma Probe (Thermo VG Scientific). The minimum beam spot diameter of the instrument is 15 μm. This is much larger than the size of a tip apex. Thus, we performed the measurements on the cantilever base with a beam spot diameter of 400 μm, which is the maximum size for this instrument.

CA measurements were performed by DM-301 (Kyowa). We used a 2 $\mu\ell$ droplet of milli-Q water for the measurements. For this measurement, we found that the surface area of the cantilever base is too small. Thus, we purchased cantilevers integrated in a Si wafer (PPP-NCHAuD-W, Nanoworld) and performed the measurements on the wafer surface.

3. Results and Discussions

3.1. SEM imaging

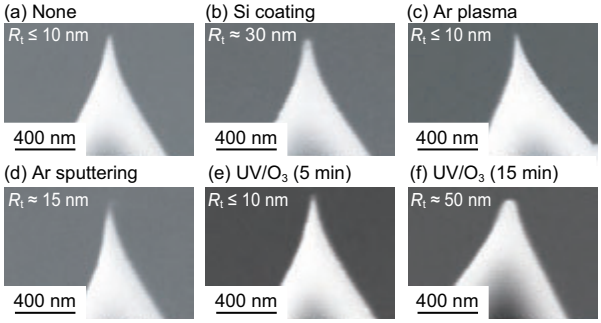

Figure 1. SEM images of the tips before and after the tip treatments.

Figure 1 shows SEM images of the tips before and after the tip treatments. Because of the limited resolution of our SEM, we were not able to accurately estimate R_t smaller than 10 nm. The SEM image shown in figure 1(a) reveals that R_t is less than 10 nm before the treatment. This sharpness is maintained even after the Ar plasma and UV/O_3 cleaning as shown in figures 1(c) and (e), respectively. The Si coating and Ar sputtering result in an increase of R_t to 30 nm (figure 1(b)) and 15 nm (figure 1(d)), respectively. This may be a serious problem for nanoscale AFM measurements where nanoscale corrugations of the surface should be accurately measured. In contrast, such slight increase of the tip radius hardly influences the atomic-scale image contrasts or short-range force profiles. This argument is supported by the experimental data shown later in this paper.

We also found that a long-term UV/O_3 cleaning results in rapid increase of R_t. For example, 15 min UV/O_3 cleaning results in an increase of R_t to 50 nm (figure 1(f)), which is much larger than that observed after the 5 min cleaning (figure 1(e)). This is probably because strong oxidation begins after 5 min UV irradiation. Due to the rapid growth of the tip size, we found it difficult to reproduce the same R_t value. Therefore, we decided to limit the cleaning time to 5 min for securing the reproducibility of R_t.

3.2. Atomic-resolution imaging

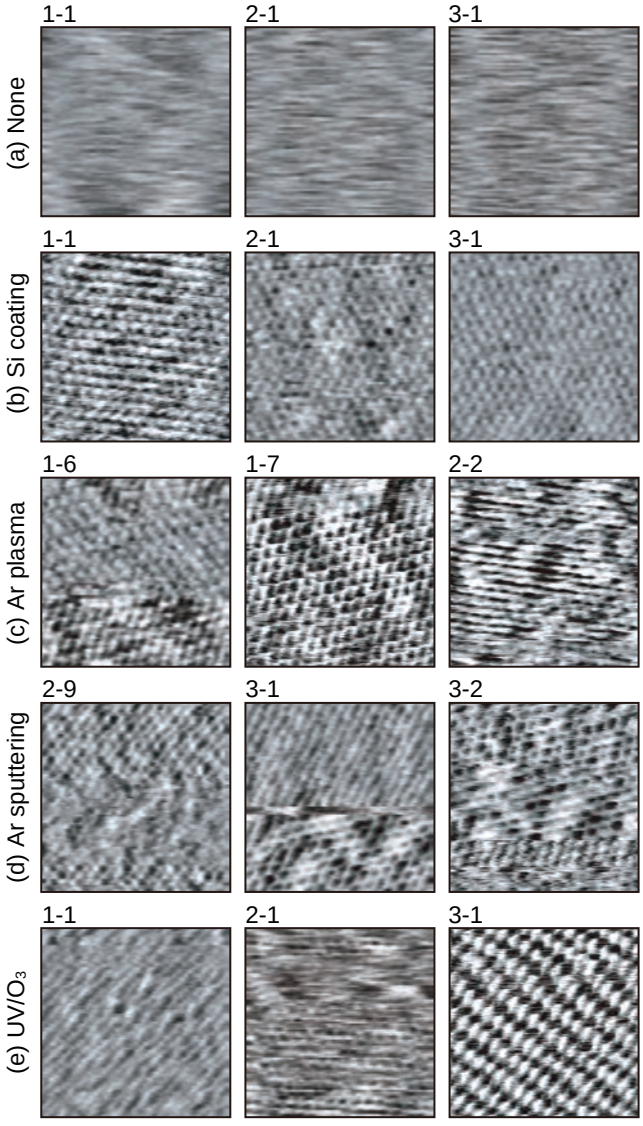

Figure 2. FM-AFM images of a cleaved mica surface obtained in PBS solution. (a) None. (b) Si coating. (c) Ar plasma. (d) Ar sputtering. (e) UV/O_3. The numbers n-m indicated in each image shows that the image corresponds to the m-th image obtained in the n-th experiment. Scan size: 8×8 nm^2. Tip velocity: 223 nm/s. $A = 0.25$ nm. $\Delta f = 800$ Hz.

We performed FM-AFM imaging of a cleaved mica surface in PBS solution with different tip treatment methods. As described above, we obtained 10 images for each experiment and we performed three experiments for each treatment method. Thus, we obtained 150 images in total. All of them are shown in Supplementary Data (figure S1). Figure 2 shows some of the examples taken from the 150 images.

Without a tip treatment, we were not able to obtain any atomic-resolution images (figure 2(a)). In contrast, with any one of the tip treatment methods, we were able to obtain an atomic-resolution image from the first scan after the tip approach. The results suggest that the apex of the as-purchased tip is covered with some contaminations and they prevent atomic-resolution imaging in liquid. Such contaminations can be removed by the tip treatments, which enables to perform an atomic-resolution imaging.

For the Si coating method, the images consistently show a similar atomic-scale contrast. For example, the first scan images of the three experiments show similar contrasts (figure 2(b)). On the contrary, the images obtained with the other methods often show a discontinuous contrast change due to a tip change (figure 2(c)-(e)). In addition, the atomic-scale contrasts observed in one experiment are significantly different from those in the other experiments (figure 2(c)-(e)). These results suggest that the tip apex condition after these treatments is not stable or reproducible. Thus, we conclude that the Si coating provides the best stability and reproducibility in an atomic-resolution imaging.

3.3. Δf curve measurements

To investigate the influence of the tip treatments on the force curve measurements, we measured 10 Δf curves with $A \simeq 0.1$ nm just after the 10 frame imaging. This amplitude is a typical value for hydration force measurements. Since we performed three experiments for each treatment method, we obtained 150 curves in total (figure S2 in Supplementary Data). Figure 3 shows the curves measured in one of the three experiments.

The curves obtained without a tip treatment show a long-range repulsive force (figure 3(a)). The tip treatments eliminate this long-range force and enable to visualize an oscillatory hydration force profile (figures 3(b)-(e)). These results suggest that the contaminations on the tip apex cause a long-range repulsive force and prevent measurements of short-range forces. This problem can be solved by any one of the tip treatment methods tested in this study.

Comparing the 10 curves obtained in one experiment (figure 3), we found some variations in the Δf profiles for any treatment methods. Such variations can be caused not only by a tip change but also by a drift of the tip position and the atomic-scale site dependence of the force profile. For the Ar plasma, Ar sputtering and UV/O_3 cleaning, the curves occasionally show a strong attractive force near the surface. In contrast, such an adhesion force is hardly observed with the Si coating method. The other results obtained with different tips show similar tendency (figure S2 in Supplementary Data).

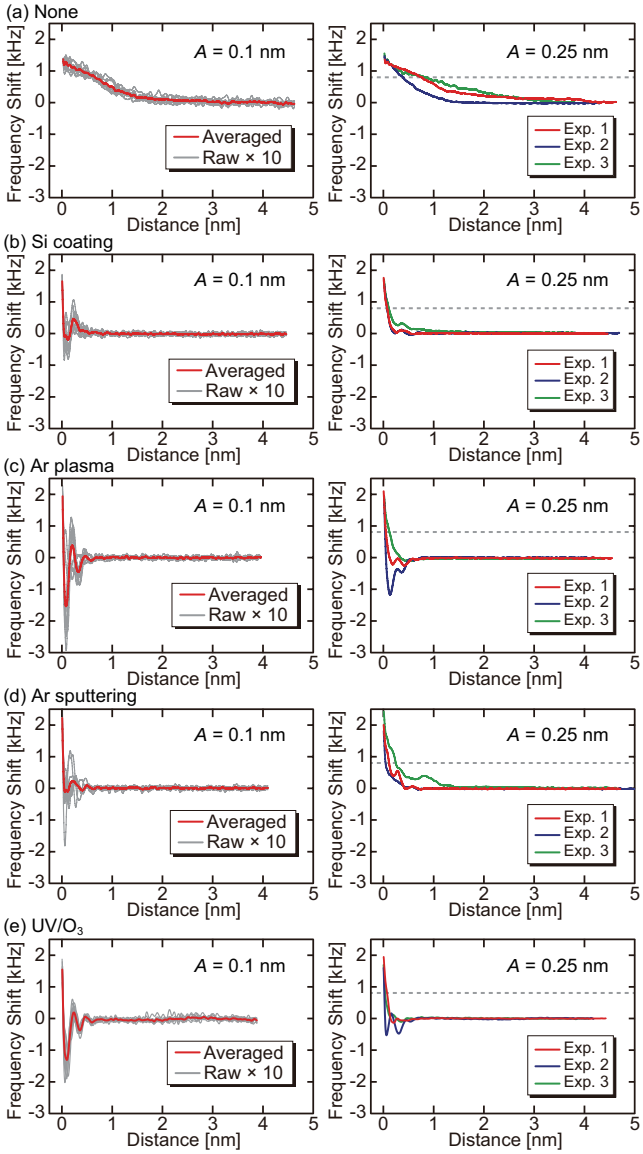

Figure 3. Δf versus distance curves measured on a cleaved mica surface in PBS solution. (a) None. (b) Si coating. (c) Ar plasma. (d) Ar sputtering. (e) UV/O_3. Tip velocity: 1 nm/s. Sample rate: 1 kHz. $B = 10$ Hz. For the curves obtained with $A \approx 0.1$ nm, we show raw data of 10 curves and their average. For those obtained with $A \approx 0.25$ nm, we show the averaged curves over 10 curves obtained in the individual experiment. The dotted lines indicate the Δf setpoint value used for the imaging experiments (figure 2).

The adhesion force may result in an atomic-scale tip crash and a tip change. This can explain the contrast changes observed during the imaging after these tip treatments (figure 2).

To clarify the relationship between the Δf profiles (figure 3) and the images (figure 2), we measured 10 Δf curves with $A \simeq 0.25$ nm. This amplitude is the same as the value used for the imaging experiments (figure 2). As we performed three experiments for each tip treatment method, we obtained 150 curves in total (figure S3 in Supplementary Data). The averaged curves obtained in the three different experiments are shown in figure 3.

We found that the difference between the 10 curves obtained in one experiment is reduced by increasing A for any treatment methods (figure S3 in Supplementary Data). One of the possible reasons is the reduced sensitivity to the short-range force that is responsible for the atomic-scale site dependence of the force profile. Another possible reason is the increased restoring force ($\simeq kA$), which may prevent an atomic-scale tip crash caused by the strong attractive force near the surface.

The averaged curves obtained in the three different experiments are significantly different except for the Si coating method (figure 3). These results show that the Si coating provides the best reproducibility in the force curve measurements. This conclusion is consistent with the one obtained from the imaging experiments.

Table 1. The slopes [kHz/nm] of the Δf versus distance curves shown in figure 3 ($A \approx 0.25$ nm) at $\Delta f = 800$ Hz. This Δf corresponds to the setpoint used for the tip-sample distance regulation during the imaging. The error range corresponds to the standard deviation of the slope values.

Exp.	None	Si coating	Ar plasma	Ar sputtering	UV/O_3
1	-0.76±0.19	-13.7±3.42	-22.6±11.9	-13.3±3.7	-59.3±16.9
2	-1.53±0.25	-11.1±1.32	-53.1±16.4	-17.7±10.3	-14.3±3.3
3	-0.98±0.67	-7.67±1.48	-10.7±2.29	-10.0±3.9	-40.1±21.4

To make a quantitative discussion on the relationship between the imaging and the Δf curves, here we analyze the slope of the Δf curves at $\Delta f = 800$ Hz (the dotted lines in figure 3). The tip-sample distance regulation during an imaging is typically operated at the repulsive branch of a Δf curve. Thus, the slope of the curves around the Δf setpoint (800 Hz in this experiment) critically influences the vertical resolution (δz) obtained in the imaging. Table 1 shows a summary of the average and standard deviation (SD) of the slope values. The results show that the slope obtained without a tip treatment is one order of magnitude smaller than those obtained with the tip treatments.

The Δf noise (δf) determined by the thermal vibration of a cantilever is given by[14]

$$\delta f = \sqrt{\frac{k_B T f_0 B}{\pi k Q A^2}}, \tag{1}$$

where k_B and T denote Boltzmann's constant and temperature, respectively. For the present experimental conditions, $\delta f \approx 30$ Hz at $B = 100$ Hz. Assuming the slope $|\partial(\Delta f)/\partial z|$ is constant, δz is given by

$$\delta z = \frac{\delta f}{|\partial(\Delta f)/\partial z|}. \tag{2}$$

True atomic-resolution imaging by AFM typically requires δz of ∼10 pm. To satisfy this condition, the slope of the Δf curve should be larger than 3 kHz/nm. According to Table 1, the slopes obtained without a tip treatment are always smaller than this value. In contrast, the slopes obtained with a tip treatment are larger than that value. These results are consistent with those obtained in the imaging experiments (figure 2).

A long-range repulsive force measured in liquid is often explained by an electric double layer force[31]. However, it is probably not the case in this experiment as we used PBS solution containing 150 mM NaCl. The Δf curves obtained without a tip treatment shows a larger noise even at a far tip position than the other curves (figure 3). This is reproducible with different tips (figures S2 and S3 in Supplementary Data). As we used the same type of cantilevers for all the experiments, such difference in the Δf noise cannot be explained by the thermal vibration of a cantilever. The results suggest that the tip apex is covered with a soft contamination layer and its fluctuation and deformation leads to an increase of a long-range repulsive force.

The averaged slope values obtained by the Si coating show smaller variations than those obtained by the other methods (table 1). This is also true of the SD of the slope values. These results confirm that the Si coating provides the best reproducibility and stability in the force curve measurements.

3.4. Origin of the fouling resistance

Table 2. Compositional ratio (Unit: %) of the cantilever base surface before and after the tip treatments estimated from the wide-range XPS spectra (figure S4 in Supplementary Data).

Element	None	Si coating	Ar plasma	Ar sputtering	UV/O_3
C	31	11	17	8	8
O	27	36	50	47	47
Si	40	52	28	44	43
Others	2	1	5	1	2

The results obtained by the imaging and the force curve measurements suggest that the effect of the tip cleaning is well maintained even after the tip transfer through the air. To understand the origin of the fouling resistance, we performed XPS measurements on the cantilever base before and after the tip treatments. From the obtained wide-range XPS spectra (figure S4 in Supplementary Data), we estimated compositional ratio of the surface (Table 2).

The C content is significantly reduced but not perfectly eliminated by the tip treatments. The result suggests that hydrocarbon contaminations are once removed by the cleaning process but adsorbed on the surface during the tip transfer process. In the meanwhile, the O content is significantly increased by the tip treatments. The result suggests that the Si surface is oxidized by the tip treatments. This should lead to an enhanced hydrophilicity.

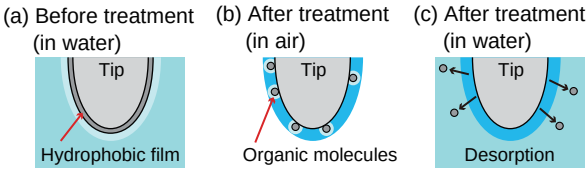

Figure 4. Schematic models to explain the origin of the fouling resistance of the cleaned tip surface.

Based on these results, we propose a model to explain the origin of the fouling resistance (figure 4). Before the tip treatments, the tip surface is covered with a contamination layer consisting of adsorbed organic molecules (figure 4(a)). Thus, the surface should be relatively hydrophobic. After the tip treatments, the hydrophobic layer is removed and the surface is oxidized to show an enhanced hydrophilicity. Thus, the surface should be covered with water even in the tip transfer process through the air (figure 4(b)). The high affinity to water molecules may reduce the adsorption of organic molecules but does not perfectly prevent it. When it is immersed in an aqueous environment, the strong hydrophilicity of the surface should lead to the formation of a stable hydration structure at the interface. This should lead to the desorption of adsorbed organic molecules. This model explains the effectiveness of the tip treatments even if we need to transfer the tip through the air.

3.5. Origin of the improved stability and reproducibility

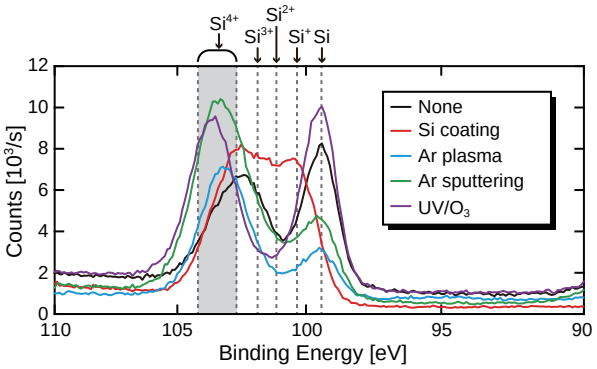

Figure 5. Si2p XPS spectra measured on a cantilever base before and after the tip treatments.

We found that the Si coating provides better stability and reproducibility in both the imaging and force measurements than the other methods. To understand the origin of the difference, we analyzed Si2p XPS spectra measured on a cantilever base before and after the tip treatments (figure 5).

Si2p spectra show different peak positions depending on the Si oxidation state (n_{Si}) as indicated by the dotted lines in figure 5. Before the tip treatments, the spectrum shows two peaks at $n_{\mathrm{Si}} = 0$ and 3–4. Thus, most of the surface Si atoms are fully oxidized to become SiO_2. According to the previous studies[23, 32, 33, 34], the surface contaminants of the tip typically come from poly(dimethylsiloxane) (PDMS) used in the cantilever storage box. As the surface before the treatment is covered with a contamination layer, we expect that some of the Si2p signal may come from the Si atoms in the adsorbed PDMS fragments.

After the Si coating, the spectrum shows a broad peak at $n_{\mathrm{Si}} = 1$–3. Thus, the surface Si atoms are partially oxidized. For AFM experiments, we immerse the tip in aqueous solution. Thus, the surface should eventually be fully oxidized by the wet process. In contrast, those obtained by the other treatment methods show two peaks at $n_{\mathrm{Si}} = 0$ and 4. In these cases, the surface Si atoms are fully oxidized by the dry processes. Thus, the surface oxidation states should not significantly be changed by the immersion into aqueous solution.

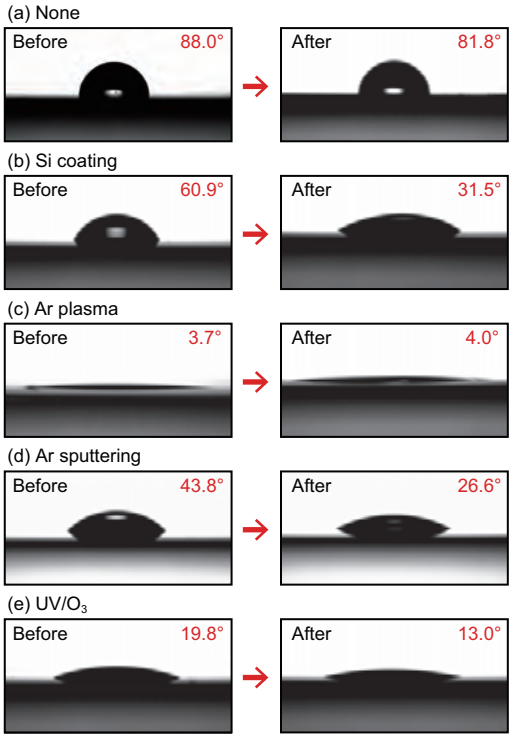

Figure 6. CAs of a 2 $\mu\ell$ water droplet on a Si wafer with and without the surface treatments. (a) None. (b) Si coating. (c) Ar plasma. (d) Ar sputtering. (e) UV/O_3. Measurements were performed before and after 10 min immersion of the wafer in pure water.

To confirm the above argument, we performed CA measurements on a Si wafer with and without the surface treatments (figure 6). We performed the measurements before and after 10 min immersion of the wafer in pure water. Without a tip treatment, the surface shows a large CA (88°), indicating its high hydrophobicity. The CA does not change significantly by the immersion in water. These results confirm that the surface before the tip treatment is covered with a hydrophobic contamination layer (figure 4(a)).

The surface after the Si coating shows a relatively high CA (60.9°). However, this value is significantly reduced to 31.5° by the immersion in water. In the meanwhile, the surface processed by the other methods show a smaller CA change. These results support our argument that the surface is oxidized by the wet process for the Si coating while it is oxidized by the dry processes for the other methods.

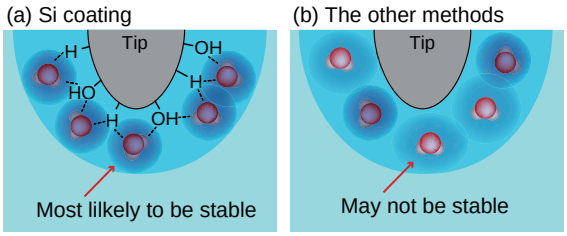

Figure 7. Schematic models showing hydration structures formed on a tip prepared by (a) the Si coating and (b) the other methods.

From these results, we conclude that the Si surface oxidized by a wet process provides better stability and reproducibility in the atomic-scale AFM measurements than that by a dry process. Here we propose one of the possible models that can explain this difference (figure 7). According to the previous infrared spectroscopy study[35], a wet oxidation of Si surface produces pairs of H and OH terminations due to the dissociative adsorption of water (figure 7(a)). This should create local spots where a stable hydration structure is formed. Thus, the hydration structure under the tip apex is likely to be stable. In contrast, the surfaces prepared by the dry oxidation mostly consist of SiO_2[35]. In this case, there is no active mechanism to create local hydration sites. Thus, the possibility of having such a stable hydration site just under the tip apex is not very high (figure 7(b)). This can explain the observed instabilities and poor reproducibility of the atomic-scale AFM measurements.

The PBS solution used in this study contains various ions such as Na^+, K^+, Cl^- and PO_4^{3-}. These ions may influence the imaging resolution and stability. In fact, we empirically know that a high-resolution imaging of three-dimensional hydration structures in water is much more difficult than that in electrolyte solution. This indicates that hydration structures both on a tip and a sample surface may be stabilized by the ions. At this stage, we have no clear explanation for the stabilization mechanism. Detailed understanding of such influence from ions should require another systematic study on the solution dependence of the AFM resolution and stability.

In this study, we focused on the experiments in an aqueous solution and found

that stable AFM measurements require not only stable tip structures but also stable hydration structures on the tip apex. As this conclusion sounds reasonable even if we replace the term "hydration" with "solvation", we speculate that a similar discussion can be made for AFM measurements in other solutions. However, the effectiveness of the tip treatment methods should be strongly dependent on the solvent and the tip material. In addition, it may be more difficult to suppress the tip contamination during the tip transfer through the air as the solvent molecules are not generally contained in ambient air.

We have been using the Si coating routinely and found that the tip maintain its stability for more than typical experimental time (3–5 hours). Therefore, its stability is sufficient for most of the applications. The chemical functionalization of the tip apex may be one of the promising ways to create stable local hydration sites. However, in this case, the tip apex must have a nanoscale protrusion consisting of a single protruded molecule supported by adjacent ones. If we can find a good way to prepare such a tip reproducibly, that may provide a better stability than the present method.

4. Conclusions

In this study, we have investigated the effect of various tip treatment methods for atomic-scale AFM imaging and force measurements in liquid. To understand the relationship between the effects observed in the AFM experiments and the surface properties, we performed XPS and CA measurements before and after the tip treatments. Major findings are summarized below.

In spite of the tip transfer through the air, all the methods provide significant improvements in both imaging and force measurements. The tip treatments not only remove surface contaminations but also enhance the hydrophilicity by surface oxidation. Although organic contaminations are adsorbed on the tip during the tip transfer through the air, they desorb from the surface when it is immersed in an aqueous environment owing to the enhanced hydrophilicity.

Among the methods tested in this study, we found that the Si coating provides the best stability and reproducibility in the atomic-scale AFM measurements. The tip surface prepared by the Si coating is oxidized when it is immersed in aqueous solution. This wet oxidation creates local spots where stable hydration structures are formed. For the other tip treatment methods, there is no active mechanism to create such local hydration sites. Thus, hydration structure formed under the tip apex is not necessarily stable.

From these results, we clarified the desirable tip properties for atomic-scale AFM measurements in liquid. First, the tip surface should be hydrophilic for keeping the clean surface during the tip transfer through the air. Secondly, not only the tip structure but also the hydration structure on the tip should be stable for stable AFM measurements.

Although we found that the Si coating is the best among the methods tested in this study, there may be other methods that can provide a better performance.

The desirable tip properties found in this study should serve as a guideline for future developments of an improved tip treatment method. The improved reproducibility and stability should enable systematic studies on various interfacial phenomena by atomic-scale AFM techniques.

Acknowledgments

This work was supported by KAKENHI (25706023), Japan Society for the Promotion of Science and ACT-C, Japan Science and Technology Agency.

References

[1] G. Binnig, C. F. Quate, and Ch. Gerber. *Phys. Rev. Lett.*, 56:930, 1986.
[2] F. Ohnesorge and G. Binnig. *Science*, 260:1451, 1993.
[3] T. Fukuma, K. Kobayashi, K. Matsushige, and H. Yamada. *Appl. Phys. Lett.*, 87:034101, 2005.
[4] B. W. Hoogenboom, H. J. Hug, Y. Pellmont, S. Martin, P. L. T. M. Frederix, D. Fotiadis, and A. Engel. *Appl. Phys. Lett.*, 88:193109, 2006.
[5] K. Suzuki, N. Oyabu, K. Kobayashi, K. Matsushige, and H. Yamada. *Appl. Phys. Express*, 4:125102, 2011.
[6] D. J. Müller, F. A. Schabert, G. Buldt, and A. Engel. 68:1681, 1995.
[7] K. H. Sheikh and S. P. Jarvis. *J. Am. Chem. Soc.*, 133:18296, 2011.
[8] H. Asakawa, S. Yoshioka, K. Nishimura, and T. Fukuma. *ACS NANO*, 6:9013, 2012.
[9] C. Leung, A. Bestembayeva, R. Thorogate, J. Stinson, A. Pyne, C. Marcovich, J. Yang, U. Drechsler, M. Despont, T. Jankowski, M. Tschöpe, and B. W. Hoogenboom. *Nano Lett.*, 12:3846, 2012.
[10] E. T. Herruzo, H. Asakawa, T. Fukuma, and R. Garcia. *Nanoscale*, 5:2678, 2013.
[11] S. Ido, K. Kimura, N. Oyabu, K. Kobayashi, M. Tsukada, K. Matsushige, and H. Yamada. *ACS NANO*, 7:1817, 2013.
[12] S. Ido, H. Kimiya, K. Kobayashi, H. Kominami, K. Matsushige, and H. Yamada. *Nat. Mater.*, 13:264, 2014.
[13] F. Hausen, J. A. Zimmet, and R. Bennewitz. *Surf. Sci.*, 607:20, 2013.
[14] T. R. Albrecht, P. Grütter, D. Horne, and D. Ruger. *J. Appl. Phys.*, 69:668, 1991.
[15] S. Morita, R. Wiesendanger, and E. Meyer, editors. *Noncontact Atomic Force Microscopy (Nanoscience and Technology)*. Springer Verlag, 2002.
[16] F. J. Giessibl. *Rev. Mod. Phys.*, 75:949, 2003.
[17] F. J. Giessibl, H. Bielefeldt, S. Hembacher, and J. Mannhart. *Appl. Surf. Sci.*, 140:352, 1999.
[18] F. J. Giessibl. *Appl. Phys. Lett.*, 76:1470, 2000.
[19] T. Fukuma, J. I. Kilpatrick, and S. P. Jarvis. *Rev. Sci. Instrum.*, 77:123703, 2006.
[20] K. Voïtchovsky, J. J. Kuna, S. A. Contera, E. Tosatti, and F. Stellacci. *Nat. Nanotech.*, 5:401, 2010.
[21] T. R. Rodoriguez and R. Garcia. *Appl. Phys. Lett.*, 84:449, 2004.
[22] T. Fukuma, K. Onishi, N. Kobayashi, A. Matsuki, and H. Asakawa. *Nanotechnology*, 23:135706, 2012.
[23] L. Sirghi, O. Kylián, D. Gilliland, G. Ceccone, and F. Rossi. *J. Phys. Chem. B*, 110:25975, 2006.
[24] M. Fujihira, Y. Okabe, Y. Tani, M. Furugori, and U. Akiba. *Ultramicroscopy*, 82:181, 2000.
[25] X. Feng, B. D. Kieviet, J. Song, P. M. Schön, and G. J. Vancso. *Appl. Surf. Sci.*, 292:107, 2014.
[26] S. Patil, G. Matei, A. Oral, and P. M. Hoffmann. *Langmuir*, 22:6485, 2006.
[27] S. H. Khan, G. Matei, S. Patil, and P. M. Hoffmann. *Phys. Rev. Lett.*, 105:106101, 2010.

[28] T. Fukuma, M. Kimura, K. Kobayashi, K. Matsushige, and H. Yamada. *Rev. Sci. Instrum.*, 76:053704, 2005.
[29] T. Fukuma and S. P. Jarvis. *Rev. Sci. Instrum.*, 77:043701, 2006.
[30] T. Fukuma. *Rev. Sci. Instrum.*, 80:023707, 2009.
[31] D. J. Müller, D. Fotiadis, S. Scheuring, S. A. Müller, and A. Engel. 76:1101, 1999.
[32] Y.-S. Lo, N. D. Huefner, W. S. Chan, P. Dryden, B. Hagenhoff, and Jr. T. P. Beebe. *Langmuir*, 15:6522, 1999.
[33] E. Bonaccurso and G. Gillies. *Langmuir*, 20:11824, 2004.
[34] B. M. Borkent, F. Mugele S. Beer, and D. Lohse. *Langmuir*, 26:260, 2009.
[35] Y. Enta, D. Shoji, M. Shinohara, M. Suemitsu, M. Niwano, N. Miyamoto, Y. Azuma, and H. Kato. *Jpn. J. Appl. Phys.*, 38S1:253, 1999.